Self-consistent determination of Hubbard U for explaining the anomalous magnetism of the Gd_{13} cluster

Kun Tao,[1,2] Jian Zhou,[1,3] Qiang Sun,[1,3] Qian Wang,[1,4] V. S. Stepanyuk,[5] and Puru Jena[1,*]

[1]*Physics Department, Virginia Commonwealth University, Richmond, Virginia 23284, USA*

[2]*Key Laboratory for Magnetism and Magnetic Materials of Ministry of Education, Lanzhou University, Lanzhou 730000, People's Republic of China*

[3]*Department of Materials Science and Engineering, Peking University, Beijing 100871, China*

[4]*Center for Applied Physics and Technology, Peking University, Beijing 100871, China*

[5]*Max-Planck-Institute of Microstructure Physics, D-06120 Halle, Germany*

(Received 2 July 2013; revised manuscript received 20 January 2014; published 5 February 2014)

The effective on-site Coulomb interaction (Hubbard U) is an important parameter for studying strongly correlated systems. While U is determined empirically by fitting to bulk values, its value for a cluster with a finite number of atoms remains uncertain. Here, we choose Gd_{13} as a prototypical example of a strongly correlated cluster. Contrary to the well-known results in transition-metal clusters where magnetic moments of clusters are *larger* than their bulk, in Gd_{13} cluster the magnetic moment is *smaller* than its bulk value. Using density functional theory and the linear response approach, we determine U self-consistently for the cluster and apply it to explain the anomalous magnetic properties of Gd_{13}. We demonstrate that the interaction between core and shell atoms of the Gd_{13} cluster strongly depends on the Hubbard U. For $U = 0$ eV magnetism is governed by a direct *f-f* electron interaction between core and shell atoms, while for $U = 5.5$ eV it is the indirect Ruderman-Kittel-Kasuya-Yosida interaction that prevails. We also demonstrate that the noncollinear spin arrangement of each atom in the cluster strongly depends on the Hubbard U. Monte Carlo calculations further confirm that magnetic moments *decrease* with temperature, thus addressing a long-standing disagreement in experimental results.

DOI: 10.1103/PhysRevB.89.085103 PACS number(s): 75.75.−c, 36.40.Cg, 65.80.−g, 75.25.Dk

I. INTRODUCTION

Density functional theory, the workhorse of modern electronic structure calculations, unfortunately, is not suitable for studying strongly correlated systems. This is traditionally accomplished by introducing to the Hohenberg-Kohn-Sham Hamiltonian an effective on-site Coulomb interaction term referred to as the Hubbard U. In this method, the electronic correlation is associated with a small number of localized orbitals which are treated in a special way. The results thus obtained strongly depend on the definition of these localized orbitals and on the choice of the interaction parameter U used in calculations. The magnitude of U can be estimated from experiments. However, the value of this parameter is uncertain for nanoparticles and clusters which are characterized by large surface-to-volume ratio, reduced coordination, low dimensionality, and symmetry. In all previous theoretical studies of magnetic clusters [1,2], alloys [3–5], magnetic molecules [6,7], and adatoms on graphene [8], the value of U is usually taken from bulk materials and assumed to be unchanged. However, it has been reported that the value of Hubbard U for an isolated atom is about three to five times larger than an atom in a bulk solid [9]. Similarly, the Hubbard U at metal and insulator surfaces was recently reported to be different from their bulk value due to the competition between surface state and effective band narrowing [10]. Although the LDA + U method has been used in a few works on strongly correlated clusters [11,12], no work on self-consistently determined U for a strongly correlated *cluster* has been reported thus far. In this paper, we present such a study by focusing on the Gd_{13} cluster, which is a prototypical strongly correlated cluster with highly localized f electrons. This choice was dictated not only because of the anomalous magnetic moment/atom of Gd_{13} which is *smaller* than its bulk value, but also to address a long-standing controversy in both experimental [13,14] and theoretical [15,16] results of its equilibrium geometry, magnetic moment, and temperature dependence. Using density functional theory with self-consistently determined U [17], which is *smaller* than its bulk value; we show that both U and spin canting are needed to explain the anomalous magnetic moment and coupling in the Gd_{13} cluster.

II. THEORETICAL METHODS

A. Density functional theory

Our calculations are based on the density functional theory (DFT) as implemented in the *Vienna ab initio simulation package* (VASP) code [18,19] with the projector augmented wave (PAW) potentials [20] and the generalized gradient approximation (GGA) due to Perdew, Burke, and Ernzerhof (PBE) [21]. For the PAW potentials the $5s$ and $5p$ semicore states have been treated as valence electrons which greatly improve the description of the valence-core exchange interaction [22]. Calculations are performed by placing the cluster at the center of a large cubic box with an edge length of 17 Å. The basis set contained plane waves with a kinetic energy cutoff of 500 eV and the total energy was converged to 10^{-6} eV. The geometry of the cluster was optimized without any symmetry constraint until all residual forces on each atom were less than 0.01 eV/Å. Several isomers were studied to determine the lowest energy configuration. Temperature dependence of magnetization was studied using Monte Carlo simulation.

*pjena@vcu.edu

B. Self-consistent determination of Hubbard U

On-site Coulomb repulsion parameter, the so-called Hubbard U, was introduced to take strong correlation into account. We note that without inclusion of Hubbard U, theory predicts the ground state of bulk Gd to be *antiferromagnetic*, while experimentally it is *ferromagnetic*. Agreement with experiment is reached once $U = 6$ eV is used for bulk Gd. Since the value of U is not known for clusters, we have used two approaches. First, we study the geometry and magnetic properties of Gd_{13} clusters as a function of U ranging from 0 to 6 eV. Second, the Hubbard U is calculated self-consistently from first principles. Different approaches have been proposed and applied to various classes of bulk materials such as pure metals, complex compounds, and superconductors [23–28]. Here, we calculate the Hubbard U based on a linear response approach that allows the parameters entering the LDA + U correction to be fixed in close relationship with the behavior of the system under consideration [17]. The method has been successfully applied to bulk materials [17] and magnetic clusters [1].

To account for the effect of strong electronic correlations we have followed the method of Anisimov and co-workers [29] by incorporating $E_{\rm Hub}$ [29] into the standard local density approximation (LDA) (or GGA) functional, namely,

$$E_{\rm LDA+U}\{[n(r)]\} = E_{\rm LDA}[n(r)] + E_{\rm Hub}\left[\left\{n^{I\sigma}_{mm'}\right\}\right] - E_{dc}[\{n^{I\sigma}\}], \quad (1)$$

where $n(r)$ is the electronic density and $n^{I\sigma}_{m}$ are the atomic orbital occupations for the "Hubbard" atom (the atom with strongly correlated orbitals) at site I. The first term $E_{\rm LDA}[n(r)]$ in Eq. (1) is the "standard" energy functional used in DFT calculations. The last term in the above equation is subtracted to avoid double counting of the interactions contained in both $E_{\rm Hub}$ and in $E_{\rm LDA}[n(r)]$. The Hubbard correction $E_U[\{n^{I\sigma}_{mm'}\}]$ is introduced to simplify the analysis and to gain a more transparent physical interpretation of "U" in standard DFT functionals

$$\begin{aligned} E_{\rm LDA+U}\{[n(r)]\} &= E_{\rm LDA}[n(r)] + E_U\left[\left\{n^{I\sigma}_{mm'}\right\}\right] \\ &= E_{\rm LDA}[n(r)] + \frac{U}{2}\sum_{I,\sigma}{\rm Tr}[n^{I\sigma}(1-n^{I\sigma})]. \end{aligned} \quad (2)$$

In the current LDA + U approach, the value of U is treated as a semiempirical parameter and is obtained by fitting different calculated physical properties to experiments. In order to calculate U self-consistently, Cococcioni and Gironcoli proposed an approach in which the total on-site occupation is considered, resulting in an effective Hubbard U [17],

$$U = \frac{d^2E^{\rm GGA}}{d(n^{If})^2} - \frac{d^2E^{\rm GGA}_0}{d(n^{If})^2}. \quad (3)$$

The second derivative of $E^{\rm GGA}_0$ is the independent electrons contribution (due to rehybridization) that has to be subtracted from the full curvature of the GGA functional.

In our paper, a number of localized potential shifts α are applied to the f levels of the Gd atoms to excite charge fluctuation on their orbitals. After solving the Kohn-Sham equations self-consistently, we get an occupation-dependent energy functional

$$E\left[\left\{n^I_f\right\}\right] = \min_{\alpha_I}\left\{E[\{\alpha_I\}] - \sum_I \alpha_I n^I_f\right\} \quad (4)$$

and

$$\frac{dE\left[\left\{n^J_f\right\}\right]}{dn^I_f} = -\alpha_I\left(\left\{n^I_f\right\}\right), \quad (5)$$

$$\frac{d^2E\left[\left\{n^J_f\right\}\right]}{d\left(n^I_f\right)^2} = -\frac{d\alpha_I\left(\left\{n^I_f\right\}\right)}{dn^I_f}. \quad (6)$$

Using α_I as the perturbation parameter, it is easy to introduce the (interacting and noninteracting) density response function of the system with respect to localized perturbations

$$\chi_{IJ} = \frac{dn^I}{d\alpha_J}, \quad \chi^0_{IJ} = \frac{dn^I_0}{d\alpha_J}, \quad (7)$$

where χ^0 is the bare response of the system, and χ is the fully interacting one. The effective interaction parameter U associated with site I can be recast as

$$U = -\frac{d\alpha^I}{dn^I_d} + \frac{d\alpha^I}{dn^I_{d0}} = \left(\chi_0^{-1} - \chi^{-1}\right)_{II}. \quad (8)$$

In the VASP code, the linear response approach has only been applied to the electric field and ionic displacements to calculate static dielectric properties, Born effective charge tensors and elastic constants, etc. However, the linear response approach to the total on-site occupation has been applied in the QUANTUM ESPRESSO (QE) code [30]. In this paper, self-consistent determination of U is performed with the QE code using GGA (PBE) exchange-correlation functional and PAW pseudopotentials. We checked the convergence of structural and electronic properties of the Gd_{13} cluster as a function of wave function and electronic density cut-off energies and arrived at the conclusion that it is enough to set them as 55 Ry and 220 Ry, respectively. The Martyna-Tuckerman correction is applied to the system for all QE calculations [31].

III. RESULTS AND DISCUSSION

A. Structure of isomers

It should be emphasized that the study of Gd clusters presents a very challenging problem because of the interplay between the geometry, charge, and spin degrees of freedom as well as the importance of strong correlation, spin-orbit coupling, and noncollinear spin alignments. To determine the relative importance of these various factors we present our results in successive steps. We begin with the results based on DFT at the GGA level without incorporating Hubbard U. Since the electronic and magnetic properties of clusters are intimately related to their geometrical structures, we first discuss the relative energies of various possible isomers of Gd_{13}. The four competing structures studied previously are hexagonal close packed (hcp), icosahedron (ICO), body centered cube (bcc), and decahedron (DEC). The optimized structures are given in Fig. 1. Among these structures we find ICO to be energetically the most favorable configuration. This is in agreement with previous calculations [16]. The energy of

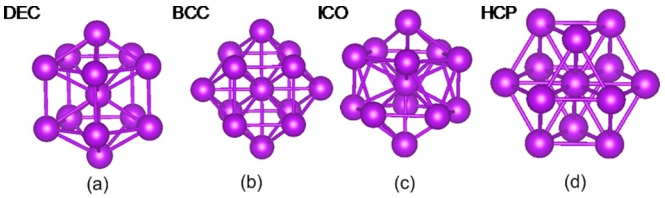

FIG. 1. (Color online) Isomers of the Gd_{13} cluster: (a) decahedron (DEC) with D_{5h} symmetry, (b) body centered cube (bcc) with O_h symmetry, (c) icosahedron (ICO) with I_h symmetry, and (d) hexagonal close packed (hcp).

DEC, bcc, and hcp structures are, respectively, 1.78, 2.58, and 2.89 eV higher than the ICO structure. The above calculations were repeated by employing the GGA + U + SOC (spin-orbit coupling) method as a function of U. The ICO structure was always found to be the most stable structure irrespective of the value of U. Consequently in all remaining calculations we only consider the ICO structure.

B. U-dependent electronic and magnetic properties

We now discuss the preferred magnetic coupling. Two different experimental values have been reported for the magnetic moment of the Gd_{13} cluster, namely, $3\mu_B$/atom [13] and 5.4 μ_B/atom [14]. Despite the obvious disagreement, it is important to note that both values are smaller than 8.82 μ_B/atom of a Gd dimer [32] and 7.63 μ_B/atom of Gd bulk [22,33,34]. This is very different from what is known about transition-metal clusters whose magnetic moments per atom are *larger* than the bulk value [35–38]. Two different explanations have been provided in the literature for this anomalous result. Using GGA-based calculations one group [16] found the central atom to be antiferromagnetically coupled to those on the shell which resulted in a reduced magnetic moment of 6.98 μ_B/atom. Another group, using a phenomenological model, attributed the reduced moment to be due to spin canting [15]. Since none of these calculations took into account the effect of strong correlation due to localized $4f$ electrons, it is difficult to judge which one of the above interpretations, if any, is valid.

To assess the effect of strong correlation on the preferred magnetic coupling, we carried out GGA + U calculations. First, we calculated the exchange energy as a function of U. For each value of U we optimized the geometry for both antiferromagnetic (the spin direction of the central atom is antiparallel to those of shell atoms) and ferromagnetic (the spin direction of the central atom is parallel to those of shell atoms) spin arrangements and calculated their energy differences, $\Delta E_{\mathrm{FM-AFM}}$. The results are plotted in Fig. 2. The most prominent feature in this figure is that preferred magnetic coupling depends strongly on U with an antiferromagnetic to ferromagnetic transition occurring between $U = 3$ and 4 eV. The energy difference becomes even larger with an increasing value of the Hubbard U due to the increased spin splitting between majority and minority spin states.

The next question is which value of the Hubbard U is an appropriate number to use for the Gd_{13} cluster? Usually, the Hubbard U is determined by seeking a good agreement between the calculated and the experiment results. However,

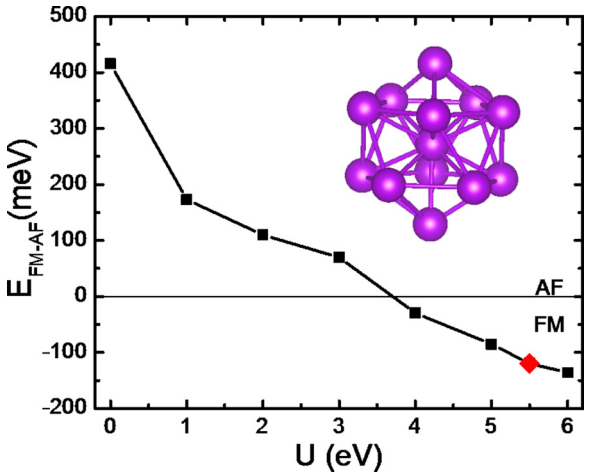

FIG. 2. (Color online) Energy difference between ferromagnetic (FM) and antiferromagnetic (AFM) states ($\Delta E_{\mathrm{FM-AFM}}$) for the Gd_{13} cluster as a function of Hubbard U. The red square represents the value of U calculated self-consistently within linear response approach. The inset in the figure is the atomic structure of the cluster with icosahedral symmetry (side view).

there are only few experiments on the Gd_{13} cluster. Here, we calculate the Hubbard U in an internally consistent manner based on the linear response method. Our self-consistently calculated value of U for the Gd_{13} cluster with ICO structure is 5.5 eV which is smaller than the bulk value of 6 eV [22]. The physical reason for this is that the coordination number in bulk Gd is 12, while in the Gd_{13} cluster it is different for the core and shell atoms, namely, 12 and 5, respectively.

In order to evaluate the effect of U on the structural, electronic, and magnetic properties of the Gd_{13} cluster, we concentrate on two cases: $U = 0$ eV and $U = 5.5$ eV. At $U = 0$ eV, the ground state is *antiferromagnetic* with the ferromagnetic state lying 0.42 eV higher in energy. This is in agreement with the previous theoretical work [16]. However, with $U = 5.5$ eV, the preferred ground state is *ferromagnetic*, which is 0.12 eV lower in energy than that of the antiferromagnetic state. When $U = 0$ eV, the bond lengths between core-shell (shell-shell) atoms in the AFM state are 3.28 (3.45) Å, while in the FM state they are 3.32 (3.49) Å. With $U = 5.5$ eV, the bond lengths between core-shell (shell-shell) atoms are 3.33 (3.50) Å for both AFM and FM states. Therefore, we conclude that the on-site Coulomb repulsion U has little effect on the geometrical parameters of the Gd_{13} cluster. This is contrary to results in Gd dimer where the bond length between FM and AFM states differs by about 0.3Å [11]. The calculated magnetic moment (in collinear alignment) of the Gd_{13} cluster is also affected very little by the inclusion of Hubbard U. For example, in the FM state, the average spin moment of the shell (core) atoms changes from 7.69 (7.25) μ_B with $U = 0$ eV to 7.77 (7.28) μ_B with $U = 5.5$ eV. In the AFM state, the magnetic moment of the shell (core) atoms changes from 7.58 (−7.07) μ_B with $U = 0$ eV to 7.79 (−7.12) μ_B with $U = 5.5$ eV. According to the Hund's rules, the half-filled $4f$ shell of the Gd atom should lead to a well localized spin-only magnetic moment and a vanishing orbital moment. It was recently pointed out that its orbital moment is

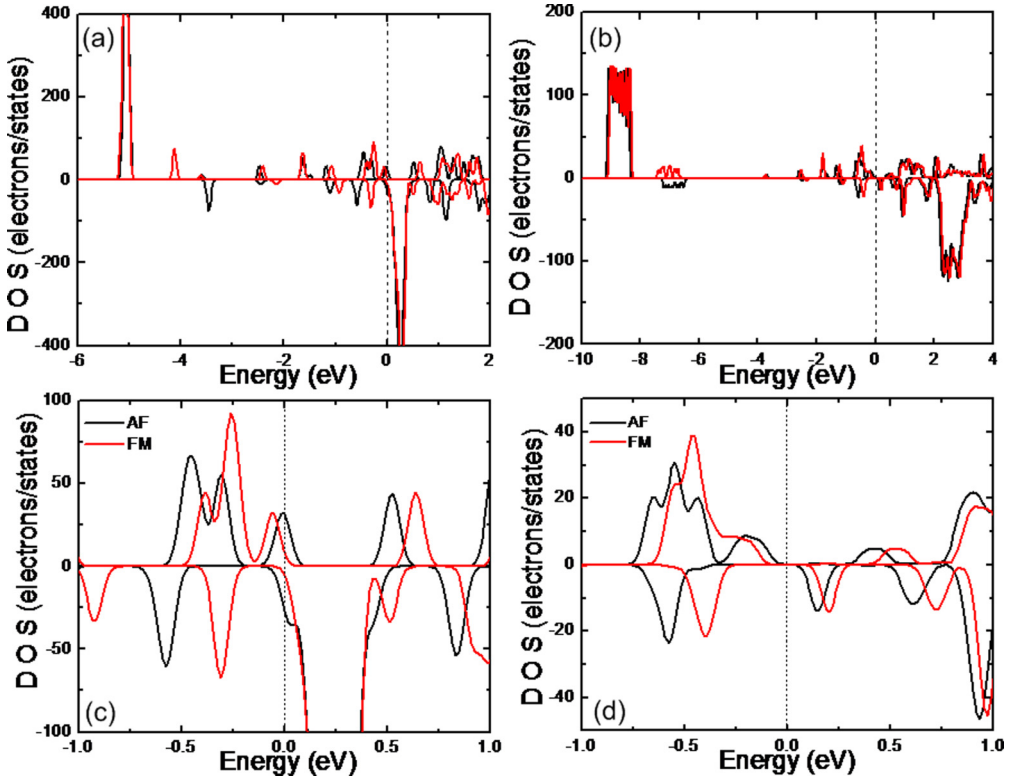

FIG. 3. (Color online) Density of states for the Gd_{13} cluster in FM and AFM configurations with different values of U: (a), (c) $U = 0$ eV; (b), (d) $U = 5.5$ eV.

not zero and large magnetic anisotropy energy is observed in scanning tunneling microscopy experiments [39]. The orbital moment of the cluster, however, shows different behavior with Hubbard U. For the AFM state with $U = 0$ eV, the orbital moment of the shell (core) atom is 0.23 (-0.007) μ_B, while it is 0.19 (-0.017) μ_B for the FM state. The orbital moment is mainly contributed by the $4f$ states. When $U = 5.5$ eV, the orbital moment of the cluster nearly vanishes. It is -0.028 (-0.024) μ_B for the shell (core) atoms for the AFM state and -0.024 (-0.006) μ_B for the FM state. The influence of Hubbard U on the orbital moment will be explained later.

The origin of the transition from the AFM state to the FM state with increasing U can be understood by analyzing the density of states (DOS) of the system. These are presented for the FM and AFM states with $U = 0$ and $U = 5.5$ eV in Fig. 3. The spin-orbit coupling does not change the energy position of $4f$ states and only results in further splitting of some states. From Fig. 3(a) we can immediately see that, with $U = 0$ eV, the majority $4f$ spin state is about 5.1 eV below the Fermi level and the minority part is about 0.2 eV above the Fermi level. Thus, the exchange splitting for $4f$ states is about 5.3 eV, which is in good agreement with previous DFT calculations for the Gd cluster [11] and bulk [22]. In Fig. 3(c), the strong peak in the minority DOS for the AFM and FM configurations is composed mainly of $4f$ states. It is weakly hybridized with $5d$ states and its tail crosses the Fermi level, giving rise to a small contribution to the orbital moment. For the majority DOS, a small peak appears at the Fermi level which is due to the hybridization between d states of the shell atoms and p states of the core atom. Note that the electronic and magnetic properties are mainly determined by $4f$ states near the Fermi level. Since they are close to the Fermi level, a direct $f-f$ coupling with an AFM state would be expected, which is consistent with our analysis of the charge redistribution in Fig. 4(a). The charge density difference $\Delta\rho_{\mathrm{AFM-FM}}$ is defined as the total charge density of AFM state $\Delta\rho_{\mathrm{AFM}}$ minus that of the FM state $\Delta\rho_{\mathrm{FM}}$. A clear $4f$ orbital character can be observed for both shell and core atoms. Compared to the FM configuration, the AFM configuration $4f$ electrons are depleted from the core atom and accumulated in the shell atoms, thus the covalent bonding between core and a shell atom is greatly increased. Therefore, a direct $f-f$ interaction between core and shell atoms in AFM configuration for the Gd_{13} cluster would be expected which would result in a lower energy than that for FM configuration.

Experiments on bulk Gd reveal that the minority $4f$ state is 4.5 eV above the Fermi level [40,41], while according to DFT calculations it is only about 0.2 eV above the Fermi level for $U = 0$ eV. This feature that all f electrons form a single peak near the Fermi level is well known in strongly correlated materials due to the failure of the density functional method [42–45]. Therefore, the location of the minority $4f$ states just above the Fermi level is unphysical, and the direct $f-f$ interaction between core and shell atoms is the origin of the incorrect prediction of the antiferromagnetic ground state for the bulk and Gd_{13} cluster.

The DOS of the FM and AFM states with $U = 5.5$ eV are plotted in Fig. 3(b). The $4f$ majority manifold is shifted down to about 8.7 eV below the Fermi level, while the minority manifold is raised up to 2.7 eV above the Fermi level resulting in an exchange splitting of $4f$ states by about 11.4 eV. This agrees with the experimental [40,41] and previous theoretical [22] results for bulk Gd very well. The large exchange splitting

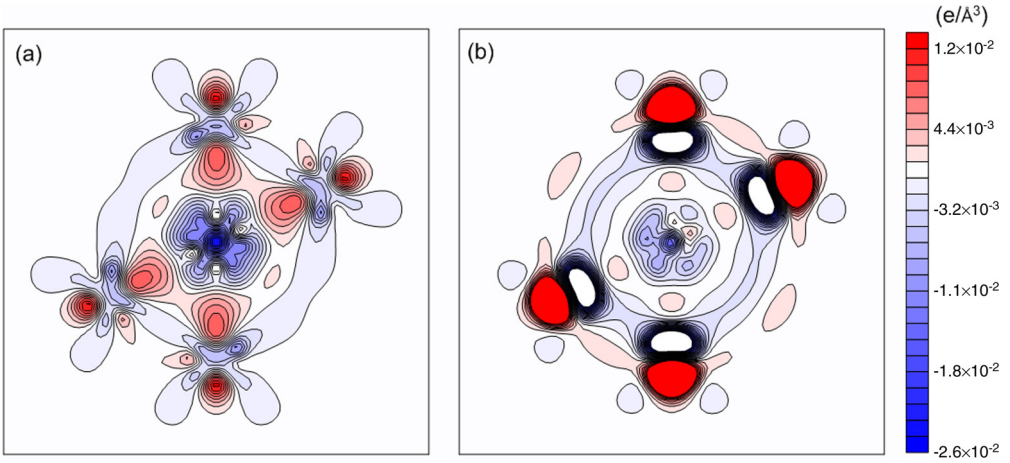

FIG. 4. (Color online) Charge density difference $\Delta\rho_{\mathrm{AFM-FM}}$ between AFM and FM configurations with different values of U: (a) $U = 0$ eV; (b) $U = 5.5$ eV.

of $4f$ states is the reason for a nearly vanishing orbital moment. Due to the large exchange splitting of $4f$ states, there is no direct $f-f$ interaction, and the electronic and magnetic properties of the cluster are mainly determined by DOS around the Fermi level.

For both configurations, as shown in Fig. 3(d), the peak in the minority spin band located about 0.2 eV above the Fermi level is mainly composed of the hybridized s and d states of shell atoms. In the majority part, the peak located around 0.25 eV below the Fermi level is due to the hybridization between p, d, and f states of core atom and d states of shell atoms. A closer look at the projected density of states on each orbital (not shown in the paper) shows that for the FM configuration the strength of the hybridization between p states and d, f states is stronger than that for the AFM configuration, which leads to a more stable configuration. It can also be observed from the charge density difference in Fig. 4(b) that the main difference between the AFM and FM configurations with $U = 5.5$ eV is dominated by p and d states. Comparing with Fig. 4(a), we find that for the AFM configuration the interaction between core and shell atoms is only slightly stronger than that for the FM configuration; the inner part of shell atoms in the FM configuration loses electrons to the outside part. In the meantime, electrons also accumulate in the area between different shell atoms. Based on these, we conclude that with $U = 5.5$ eV the strength of the interaction between core and shell atoms for AFM is nearly the same as that for the FM configuration, while the coupling between shell atoms is increased in the FM configuration. This makes the FM configuration energetically more favorable than that of the AFM state. Therefore, with the on-site Coulomb repulsion U, there is no direct $f-f$ electron interaction between core and shell atoms because they are far away from the Fermi energy, but polarized p and d electrons mediate the coupling between localized $4f$ electrons. This indirect interaction is the so-called Ruderman-Kittel-Kasuya-Yosida (RKKY) -type exchange interaction, which is a well-known mechanism for explaining the exchange interaction in rare-earth materials. For the Gd_{13} cluster we emphasize that the Hubbard U plays a vital role in determining the interaction between core and shell atoms: For $U = 0$ eV magnetism is governed by direct $f-f$ electron interaction between core and shell atoms, while for $U = 5.5$ eV it is the indirect RKKY interaction that prevails.

C. Charge redistribution with U

To get further insight into the effect of on-site Coulomb repulsion U, we have analyzed the charge density of the cluster and in particular the charge transfer between the core and shell atoms in AFM and FM states with different values of U. In the AFM state with $U = 0$ eV, we find that there is small excess charge in d, s, and p states, while there is small depletion of charge in f states with $U = 5.5$ eV. Similar results were also found for the FM state. It is to be pointed out that even small changes in valence electrons can have a significant effect on the exchange coupling of the system. In Fig. 5 we plot isosurfaces

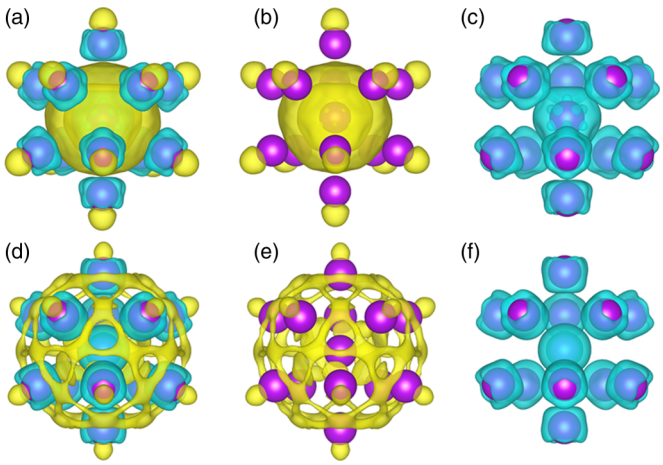

FIG. 5. (Color online) Isosurfaces (isovalue of 0.003 electron/Å^3) of total charge density difference between $U = 5.5$ eV and $U = 0$ eV for AFM configuration (upper panel) and FM configuration (lower panel). Yellow and blue represent positive and negative charge density difference, respectively. (a) Total charge density difference for the AFM state. (b) Excess charge and (c) depletion charge for the AFM state. (d) Total charge density difference for the FM state. (e) Excess charge and (f) depletion charge for the FM state.

of charge density difference $\Delta\rho_{5.5-0}$ between $U = 5.5$ eV and $U = 0$ eV for the AFM and FM configurations, keeping the same geometrical structure in all cases. As shown in Fig. 5(a), for the AFM state, with an increasing U, charges from both core and shell atoms flow to the center area and increase their covalent character. For the FM state, as shown in Fig. 5(d), both core and shell atoms lose electrons and most of the excess charge accumulates between the shell atoms—characteristic of the metallic nature of bonding. This means that due to an excess of s, p, and d electrons, the metallic interactions between shell atoms increase. Therefore, we conclude that with increasing Hubbard U, the metallic character of the cluster strongly increases for the FM state. Consequently, the coupling between Gd atoms is indirect and is mediated via their valence electrons. This is consistent with our analysis of DOS in Fig. 3 that the indirect RKKY interaction plays an important role in determining the magnetic ground state of the Gd_{13} cluster.

D. Noncollinear configurations

Up to now, all of our results are based on collinear spin calculations. The average magnetic moment of the Gd_{13} cluster obtained at this level is more than 7 μ_B, which is significantly larger than the experimental values [13,14]. A possible reason for this discrepancy could be that spins are not collinear. Although many works on noncollinear spin configurations for transition-metal clusters with d electrons have been carried out [46–51], only few have been performed for rare-earth clusters [52–54]. As mentioned in the above, a phenomenological model based on the Heisenberg model and RKKY-like interaction considered noncollinear spin configurations [15]. However, these authors predicted the lowest energy structure of Gd_{13} to have hcp symmetry, which does not agree with our as well as previous results [16]. It is well known that the LDA method cannot effectively deal with a highly correlated system. Using the GGA + U + SOC method, we have investigated tens of possible noncollinear spin configurations for the cluster.

In Stern-Gerlach experiment the z component of the total magnetization is measured. In the following part, we will concentrate on the magnetic moment along the z direction. Because the ground state for the Gd_{13} cluster for $U = 0$ eV is *antiferromagnetic*, we first searched for its noncollinear spin configuration. A stable configuration is shown in Fig. 6(a). In this configuration, the magnetic moments along the z direction for shell atoms are between 6.98 μ_B and 7.43 μ_B. For the core atom it is 6.67 μ_B and its spin direction is antiparallel to those of the shell atoms. This is summarized in Table I. The average magnetic moment along the z direction for the cluster is 6.1 μ_B, which is still larger than the experimental value [13,14].

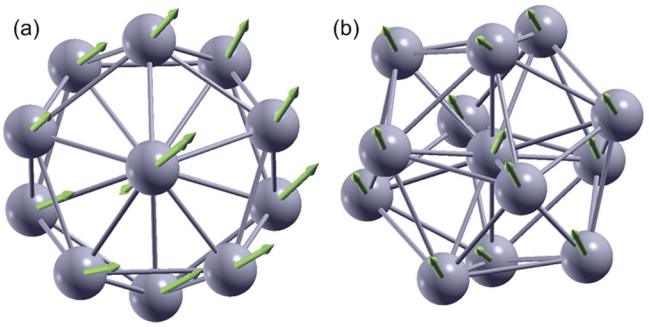

FIG. 6. (Color online) Noncollinear spin configurations of the Gd_{13} cluster for two configurations: (a) AFM state with $U = 0$ eV. (b) FM state with $U = 5.5$ eV.

TABLE I. Cartesian coordination (in Å) of the Gd_{13} cluster and magnetic moments (in μ_B) for each atom in three directions as $U = 0$ eV.

x	y	z	M_x	M_y	M_z
8.500	8.499	11.824	1.734	1.322	7.239
11.323	9.416	9.985	1.271	1.860	7.200
8.495	11.472	9.989	1.422	1.507	7.260
5.674	9.421	9.989	1.000	0.876	7.427
6.757	6.096	9.985	1.900	0.351	7.287
10.251	6.092	9.983	2.097	1.168	7.155
8.500	8.498	8.501	−1.589	−1.249	−6.674
10.240	10.904	7.015	1.172	2.040	7.165
6.749	10.908	7.017	1.552	1.099	7.304
5.678	7.584	7.014	2.013	0.823	7.226
8.505	5.528	7.010	2.231	1.174	7.117
11.326	7.579	7.010	2.121	1.904	6.986
8.500	8.502	5.176	2.109	1.615	7.082

With $-U = 5.5$ eV, the ground state of the cluster is *ferromagnetic*. The energetically most favorable noncollinear spin configuration is shown in Fig. 6(b). The z components of the magnetic moments of shell atoms lie in the range of 5.39–5.48 μ_B, and it is 4.35 μ_B for the core atom which is parallel to shell atoms, summarized in Table II. The average magnetic moment of the cluster is 5.35 μ_B, which agrees very well with the experimental result of 5.4 μ_B [14]. Thus, we conclude that both U and spin canting are necessary to account for the reduced magnetic moment of the Gd_{13} cluster.

E. Temperature dependence

We next explored the temperature dependent magnetic behavior of the Gd_{13} cluster with ICO structure using Monte

TABLE II. Cartesian coordination (in Å) of the Gd_{13} cluster and magnetic moments (in μ_B) for each atom in three directions as $U = 5.5$ eV.

x	y	z	M_x	M_y	M_z
8.500	8.499	11.824	4.016	3.812	5.395
11.323	9.416	9.985	3.904	3.851	5.450
8.495	11.472	9.989	4.124	3.568	5.482
5.674	9.421	9.989	3.894	3.866	5.445
6.757	6.096	9.985	3.992	3.798	5.420
10.251	6.092	9.983	3.970	3.799	5.437
8.500	8.498	8.501	4.161	4.004	4.347
10.240	10.904	7.015	3.987	3.796	5.428
6.749	10.908	7.017	3.977	3.788	5.441
5.678	7.584	7.014	3.926	3.832	5.448
8.505	5.528	7.010	4.119	3.573	5.480
11.326	7.579	7.010	3.924	3.848	5.436
8.500	8.502	5.176	4.011	3.803	5.406

Carlo simulation. As mentioned before one experimental group reported the magnetic moment of the cluster to *increase* with temperature [13], while the other group argued that it *decreases* with temperature [14]. Monte Carlo simulations based on the Heisenberg model have been carried out earlier to investigate the temperature dependent magnetism of the Gd_{13} cluster [52]. However, these studies used the hcp structure for the Gd_{13} cluster which, as we have shown, is *not* the ground state geometry.

In this paper, we chose the ICO structure and use three configurations to explore the magnetic coupling between the shell and core Gd atoms. The first one is the ground state with all the spins coupled ferromagnetically. In the second configuration, the spin of the central Gd atom is antiparallel to the shell atoms. Reversing the spin of another apex atom gives us a third configuration. For simplicity, we assume that the magnetic behavior of all the shell Gd atoms are the same as the apex Gd atom. We denote the energies of the three configurations as E_1, E_2, and E_3, respectively, and the magnetic coupling exchange parameters between the shell Gd atoms and the core-shell atoms as J_{sc} and J_{ss}. According to the Ising model the energies can be explicitly expressed as follows:

$$E_1 - E_0 = 12J_{sc}m_s m_c + 30J_{ss}m_s m_s, \tag{9}$$

$$E_2 - E_0 = -12J_{sc}m_s m_c + 30J_{ss}m_s m_s, \tag{10}$$

$$E_3 - E_0 = 10J_{sc}m_s m_c + 20J_{ss}m_s m_s, \tag{11}$$

where E_0 is the total energy excluding the magnetic coupling of the Gd_{13} cluster, and m_c and m_s are the magnetic moments of the core and shell Gd atoms, respectively. The coefficient 12 in Eqs. (9) and (10) indicates that there are 12 atoms on the shell magnetically interacting with the core Gd atom. Positive and negative signs represent the ferromagnetic and antiferromagnetic couplings, respectively. The coefficient 30 in Eqs. (9) and (10) represent 30 ferromagnetic interactions among the shell atoms. In Eq. (11), as one apex Gd atom aligns antiparallel with other atoms, the interactions between the shell and the core atoms then contain 11 ferromagnetic and one antiferromagnetic couplings, resulting in ten total effective interactions. Similarly, as five shell atoms change from ferromagnetic to antiferromagnetic coupling, only 20 effective interactions remain. J_{sc} and J_{ss} values are calculated to be -0.104 and -0.874 meV, respectively. The negative sign indicates ferromagnetic coupling. It can be seen that magnetic coupling between the shell atoms is stronger than that between the core and the shell atom. This is because the bond length between the shell atoms is shorter than that between the shell and core atom.

For each temperature we used 1×108 trial steps to find the equilibrium state, and then 1×107 steps were performed to calculate the average magnetic moment. Longer steps had only marginal influence on the final results. The simulations below 1000 K are shown in Fig. 7. Below 130 K, the magnetic moments are nearly constant. Above 130 K, the spin of the core Gd atom starts to change, while the moments of the shell atoms retain their values and the total magnetic moment decreases. Above 220 K, the shell magnetic moments also begin to decrease. As the temperature increases above 660 K we find that some antiparallel configurations appear in the equilibrium states and the total magnetic moment decreases sharply. This agrees with the experimental observation of Gerion *et al.* [14].

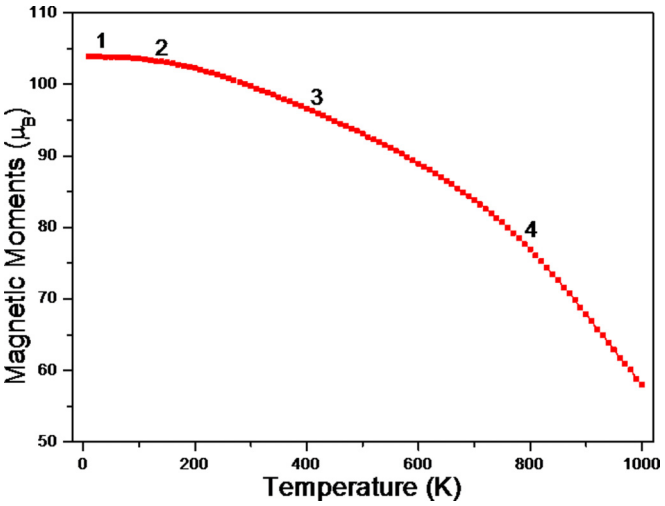

FIG. 7. (Color online) Variation of the magnetization of the Gd_{13} cluster as a function of temperature. The numbers 1, 2, 3, and 4 indicate four different temperatures where simulations were performed.

IV. CONCLUSION

In conclusion, using density functional theory and linear response approach we have determined the Hubbard U self-consistently for the strongly correlated Gd_{13} cluster. We demonstrate that the value of U for cluster is smaller than its bulk value due to its reduced coordination number. Hubbard U dependent geometry structure for different isomers has been carefully checked, and the ICO is always found to be the most stable structure, irrespective of the value of U. Based on this structure, we investigate the electronic and magnetic properties as a function of Hubbard U. For $U = 0$ eV, magnetism is governed by direct f-f electron interaction between core and shell atoms. This unphysical result is due to the limitation of the density functional theory. For $U = 5.5$ eV, the interaction is governed by the indirect RKKY mechanism. Furthermore, in collinear configuration, the spin of the core atom is antiparallel to that of the shell atom for $U = 0$ eV, while it is parallel for $U = 5.5$ eV. Noncollinear calculations reveal that the spin configuration strongly depends on the Hubbard U and the magnetic moment of the cluster for $U = 5.5$ eV agrees very well with the experimental results. The temperature dependent magnetic properties are studied with Monte Carlo simulations. The quantitative agreement between the calculated and experimental magnetic moment and the temperature dependence of the Gd_{13} cluster underscores the need for self-consistent determination of Hubbard U for strongly correlated systems and the importance of spin canting. These effects are expected to be important not only for other rare-earth clusters in the gas phase but also for those deposited on different substrates or embedded in different environments.

ACKNOWLEDGMENTS

This work is supported by the US Department of Energy, Office of Basic Energy Sciences, Division of Materials Sciences and Engineering under Award No. DE-FG02-96ER45579. K.T is also partially supported by the National Natural Science Foundation of China (Grant No. NSFC-11274146), the National Basic Research Program of China (Grant No. 2012CB933101), and the Fundamental Research Funds for the Central Universities (Grant No. 2022013zrct01). Resources of the National Energy Research Scientific Computing Center supported by the Office of Science of the US Department of Energy under Contract No. DE-AC02-05CH11231 are also acknowledged.

[1] F. Filippone, G. Mattioli, P. Alippi, and A. A. Bonapasta, Phys. Rev. Lett. **107**, 196401 (2011).
[2] A. Migani, K. M. Neyman, F. Illas, and S. T. Bromley, J. Chem. Phys. **131**, 064701 (2009).
[3] D. W. Boukhvalov, V. V. Dobrovitski, M. I. Katsnelson, A. I. Lichtenstein, B. N. Harmon, and P. Kogerler, Phys. Rev. B **70**, 054417 (2004).
[4] U. del Pennino, V. Corradini, R. Biagi, V. De Renzi, F. Moro, D. W. Boukhvalov, G. Panaccione, M. Hochstrasser, C. Carbone, C. J. Milios, and E. K. Brechin, Phys. Rev. B **77**, 085419 (2008).
[5] C. D. Pemmaraju, I. Rungger, and S. Sanvito, Phys. Rev. B **80**, 104422 (2009).
[6] A. K. Pathak, D. Paudyal, Y. Mudryk, K. A. Gschneidner, Jr., and V. K. Pecharsky, Phys. Rev. Lett. **110**, 186405 (2013).
[7] A. B. Shick and O. N. Mryasov, Phys. Rev. B **67**, 172407 (2003).
[8] T. O. Wehling, A. I. Lichtenstein, and M. I. Katsnelson, Phys. Rev. B **84**, 235110 (2011).
[9] J. Zaanen and G. A. Sawatzky, J. Solid State Chem. **88**, 8 (1990).
[10] E. Şaşioğlu, C. Friedrich, and S. Blügel, Phys. Rev. Lett. **109**, 146401 (2012).
[11] G. Kim, Y. Park, M. JoonHan, J. Yu, C. Heo, and Y. Hee Lee, Solid State Commun. **149**, 2058 (2009).
[12] M. Joon Han, T. Ozaki, and J. Yu, Chem. Phys. Lett. **492**, 89 (2010).
[13] D. C. Douglass, J. P. Bucher, and L. A. Bloomfield, Phys. Rev. Lett. **68**, 1774 (1992).
[14] D. Gerion, A. Hirt, and A. Châtelain, Phys. Rev. Lett. **83**, 532 (1999).
[15] D. P. Pappas, A. P. Popov, A. N. Anisimov, B. V. Reddy, and S. N. Khanna, Phys. Rev. Lett. **76**, 4332 (1996).
[16] H. K. Yuan, H. Chen, A. L. Kuang, and B. Wu, J. Chem. Phys. **135**, 114512 (2011).
[17] M. Cococcioni and S. de Gironcoli, Phys. Rev. B **71**, 035105 (2005).
[18] G. Kresse and J. Hafner, Phys. Rev. B **47**, 558 (1993).
[19] G. Kresse and J. Furthmuller, Phys. Rev. B **54**, 11169 (1996).
[20] P. E. Blöchl, Phys. Rev. B **50**, 17953 (1994).
[21] J. P. Perdew, K. Burke, and M. Ernzerhof, Phys. Rev. Lett. **77**, 3865 (1996).
[22] M. Petersen, J. Hafner, and M. Marsman, J. Phys.: Condens. Matter **18**, 7021 (2006), and references therein.
[23] T. Kotani, J. Phys.: Condens. Matter **12**, 2413 (2000).
[24] I. Schnell, G. Czycholl, and R. C. Albers, Phys. Rev. B **65**, 075103 (2002).
[25] I. V. Solovyev and M. Imada, Phys. Rev. B **71**, 045103 (2005).
[26] K. Nakamura, R. Arita, Y. Yoshimoto, and S. Tsuneyuki, Phys. Rev. B **74**, 235113 (2006).
[27] F. Aryasetiawan, K. Karlsson, O. Jepsen, and U. Schönberger, Phys. Rev. B **74**, 125106 (2006).
[28] P. Werner, M. Casula, T. Miyake, F. Aryasetiawan, A. J. Millis, and S. Biermann, Nat. Phys. **8**, 331 (2012).
[29] V. I. Anisimov, J. Zaanen, and O. K. Andersen, Phys. Rev. B **44**, 943 (1991).
[30] P. Giannozzi, S. Baroni, N. Bonini, M. Calandra, R. Car, C. Cavazzoni, D. Ceresoli, G. L. Chiarotti, M. Cococcioni, I. Dabo, A. Dal Corso, S. de Gironcoli, S. Fabris, G. Fratesi, R. Gebauer, U. Gerstmann, C. Gougoussis, A. Kokalj, M. Lazzeri, L. Martin-Samos, N. Marzari, F. Mauri, R. Mazzarello, S. Paolini, A. Pasquarello, L. Paulatto, C. Sbraccia, S. Scandolo, G. Sclauzero, A. P. Seitsonen, A. Smogunov, P. Umari, and R. M. Wentzcovitch, J. Phys.: Condens. Matter **21**, 395502 (2009).
[31] G. J. Martyna and M. E. Tuckerman, J. Chem. Phys. **110**, 2810 (1999).
[32] L. W. Roeland, G. J. Cock, F. A. Muller, A. C. Moleman, K. A. McEwen, R. G. Jordan, and D. W. Jones, J. Phys. F: Met. Phys. **5**, L233 (1975).
[33] R. J. van Zee, S. Li, and W. Weltner, Jr., J. Chem. Phys. **100**, 4010 (1994).
[34] Ph. Kurz, G. Bihlmayer, and S. Blügel, J. Phys.: Condens. Matter **14**, 6353 (2002).
[35] J. Bansmann, S. H. Baker, C. Binns, J. A. Blackman, J.-P. Bucher, J. Dorantes-Dávila, V. Dupuis, L. Favre, D. Kechrakos, A. Kleibert, K.-H. Meiwes-Broer, G. M. Pastor, A. Perez, O. Toulemonde, K. N. Trohidou, J. Tuaillon, and Y. Xie, Surf. Sci. Rep. **56**, 189 (2005).
[36] J. P. Bucher, D. C. Douglass, and L. A. Bloomfield, Phys. Rev. Lett. **66**, 3052 (1991).
[37] B. K. Rao and P. Jena, Phys. Rev. Lett. **89**, 185504 (2002).
[38] M. R. Press, F. Liu, S. N. Khanna, and P. Jena, Phys. Rev. B **40**, 399 (1989).
[39] T. Schuh, T. Miyamachi, S. Gerstl, M. Geilhufe, M. Hoffmann, S. Ostanin, W. Hergert, A. Ernst, and W. Wulfhekel, Nano. Lett. **12**, 4805 (2012).
[40] J. K. Lang, Y. Baer, and P. A. Cox, J. Phys. F: Met. Phys. **11**, 121 (1981).
[41] J. E. Ortega, F. J. Himpsel, Dongqi Li, and P. A. Dowben, Solid State Commun. **91**, 807 (1994).
[42] M. Richter, J. Phys. D **31**, 1017 (1998).
[43] M. Diviš, K. Schwarz, P. Blaha, G. Hilscher, H. Michor, and S. Khmelevskyi, Phys. Rev. B **62**, 6774 (2000).
[44] L. Perit, A. Svane, Z. Szotek, P. Strange, H. Winter, and W. M. Temmerman, J. Phys.: Condens. Matter **13**, 8697 (2001).
[45] S. J. Asadabadi, S. Cottenier, H. Akbarzadeh, R. Saki, and M. Rots, Phys. Rev. B **66**, 195103 (2002).
[46] L. Fernandez-Seivane and J. Ferrer, Phys. Rev. Lett. **99**, 183401 (2007).

[47] P. Ruiz-Díaz, J. L. Ricardo-Chávez, J. Dorantes-Dávila, and G. M. Pastor, Phys. Rev. B **81**, 224431 (2010).
[48] S. Sahoo, A. Hucht, M. E. Gruner, G. Rollmann, P. Entel, A. Postnikov, J. Ferrer, L. Fernández-Seivane, M. Richter, D. Fritsch, and S. Sil, Phys. Rev. B **82**, 054418 (2010).
[49] P. Błoński, S. Dennler, and J. Hafner, J. Chem. Phys. **134**, 034107 (2011).
[50] P. Błoński and J. Hafner, J. Chem. Phys. **134**, 154705 (2011).
[51] M. Tanveer, P. Ruiz-Díaz, and G. M. Pastor, Phys. Rev. B **87**, 075426 (2013).
[52] V. Z. Cerovski, S. D. Mahanti, and S. N. Khanna, Eur. Phys. J. D **10**, 119 (2000).
[53] L. Hernández and C. Pinettes, J. Magn. Magn. Mater. **295**, 82 (2005).
[54] F. López-Urías, A. Díaz-Ortiz, and J. L. Morán-López, Phys. Rev. B **66**, 144406 (2002).